International Research Journal of Innovations in Engineering and Technology (IRJIET)

ISSN (online): 2581-3048

Volume 6, Issue 11, pp 12-24, November-2022

https://doi.org/10.47001/IRJIET/2022.611002

The Effect of Outlet Diameter and Shape of Vortex Finder on the Efficiency of a Square Cyclone

[1]*Abdul Basit, [2]Mohamad Said Kartono Tony Suryo Utomo, [3]Eflita Yohana, [4]Vika Abidah, [5]Kwang-Hwan Choi

[1,2,3]Department of Mechanical Engineering, Diponegoro University, Jl. Prof. Sudharto, SH, Semarang 50275, Indonesia
[4]Department of Physics, Diponegoro University, Jl. Prof. Sudharto, SH, Semarang 50275, Indonesia
[5]College of Engineering Pukyong National University, 365 Sinseon-Ro, Nam-Gu, Busan 608-739, Republic of Korea
*Corresponding Author's E-mail: basitmoedikal05@gmail.com

***Abstract* - The cyclone separator has a simple construction design, low operating cost, and the ability to adapt to high pressure and temperature conditions, making it widely used in industry. Cyclone performance can be seen from the efficiency of particle collection and pressure drop. Computational Fluid Dynamic (CFD) methods are widely used in solving complex flow problems. This study examines the outlet diameter and modification of the shape of the vortex finder on the performance of a square cyclone to increase the efficiency of separating a square cyclone. Four different forms of vortex finder, Standard Vortex (SV), Convergent Vortex (CV), Divergent Vortex (DV), and Convergent Divergent Vortex (CDV) will be simulated to assess the impact of gas temperature on the performance of the square cyclone in the velocity flow plane, cyclone performance, temperature distribution, and heat transfer. The RSM turbulence model is used to simulate fluid flow. The Eulerian-Langrangian approach was chosen to predict the phase motion of the particles. The trajectories of particles in the stream are tracked individually using the DPM method. The simulation results show that the use of the Convergent Divergent Vortex (CDV) form increases the efficiency of square cyclone separation while at the same time increasing the pressure drop. Using a Convergent Vortex (CV) shape is useful for reducing the size of the piece by up to 50%. This is because the incoming air flow experiences centrifugal force in the vortex finder area, thereby increasing efficiency and increasing the pressure drop on the square cyclone.**

Keywords: CFD, Square Cyclone, Vortex Finder, Pressure Drop, Efficiency.

I. INTRODUCTION

A gas cyclone separator is equipment used to separate particulates from a gas stream by applying centrifugal force. Many industrial processes use cyclones to separate particulates in their production processes. Cyclones have various uses in the industrial world ranging from the chemical industry, food processing, pharmaceuticals, and all types of industries that involve particle separation [1-3]. In addition, cyclones are specifically used to separate air pollution particles in many industries. Compared with other types of particulate separators, cyclone separators have a simple construction design [1][4], [5] easy to operate and maintain [6] [7], low power consumption, capable of being used in extreme operating conditions (high temperature, high pressure, and corrosive gases) [8-9]. Many studies have been carried out to understand the effect of different geometric and operating parameters on the performance and fluid dynamics in the cyclone separator. Therefore, it is suitable for continuous use.

One of the characteristics of cyclones is the presence of free eddies and forced eddies, more commonly known as Rankine eddies [10–12]. The complexity of the cyclone separator flow pattern is often a problem in theoretical and experimental studies [13]. The rapid development of technology encourages researchers to use Computational Fluid Dynamic (CFD) in solving cyclone separator simulation cases because it can predict fluid flow characteristics, particle trajectories and pressure drop in cyclones, in addition to saving costs and time [14-17]. The transient simulation method is commonly used in simulating the flow in a cyclone. This is because the steady method shows an inability to interpret the physical phenomena that occur in cyclones, namely the formation of Precessing Vortex Core (PVC) or vortex flow instability [18]. Griffiths and Boysan [14] in their research explained that the key to the success of turbulent flow modeling lies in the selection of a turbulent model. Various turbulent models are available in fluent software to describe flow behavior. Standard model $k-\varepsilon$, $k-\varepsilon$ realizable, and RNG $k-\varepsilon$ not recommended for strong eddy currents due to the assumption of an isotropic turbulent structure in their formulation, as found in cyclones [19]. The Turbulent Reynold Stress Model (RSM) is the preferred choice of researchers in simulating cyclone flow [20-22] because of the ability of this turbulent model to predict vortex flow patterns and produce simulations that are close to reality with shorter and lower time. Computer capacity of the Large Eddy Simulation (LES) model [23-25].

International Research Journal of Innovations in Engineering and Technology (IRJIET)

ISSN (online): 2581-3048

Volume 6, Issue 11, pp 12-24, November-2022

https://doi.org/10.47001/IRJIET/2022.611002

Conventional cyclone separators are cylindrical in shape with a cone at the bottom, widely applied as gas and particle separators in FBD (Fluid Bed Dryer) boiler machines. The main drawbacks of conventional cyclones (with a circular cross section) are the large volume and thick refractory layer, which is responsible for long start and stop times. [26] in addition, the increased intake gas decreased at the tangential velocity. An alternative to overcome this problem is to use a square cyclone separator [27] [28]. Square cyclones have additional advantages over conventional cyclones, including easy construction, shorter start-stop times, and more importantly, easy integration with boilers [29]. According to the report [30] regarding the comparison of the performance of conventional cyclones with square cyclones from the simulation results, square cyclones performed better when viewed from the point of view of pressure drop. [31] Conducted experimental and numerical experiments on gas and solid separators in a square cyclone separator applied to a CFB machine and showed the separation efficiency results were as good as conventional cyclones. [32] also solved the experimental and numerical problems of gas-solid separators, in which the conical and space sections were replaced by square shapes. Compared to conventional cyclone separators, the new geometry shows advantages in performance, such as smaller pressure drop. The pressure drop increases by an average of 10% when the particles are injected into the stream of low concentration. To improve the performance of square cyclones, it is necessary to innovate in cyclone geometry. [33]. [23] simulated the impact of different diameters of a vortex finder on the flow plane and efficiency of the cyclone. In their study, fifteen configurations of the vortex finder were investigated. Their results show that the geometric shape of the vortex finder has a great influence on the particle separation efficiency of the cyclone separator [34]. [24] Numerically studied the performance of square cyclones by changing their geometric parameters by optimization methods and validating their results with experimental data. They found that the optimal square cyclone resulted in much higher performance. Also, [29] and [25] carried out a numerical investigation of a new design for a square cyclone to improve its separation efficiency. They showed that a square cyclone with a convergent vortex finder can increase the pressure in the vortex finder region. In addition, the shape of the vortex finder has an effect on the tangential velocity of the square cyclone. The geometry of this vortex finder can overcome the tangential velocity which decreases as the intake air temperature increases.

It is not easy to increase efficiency and reduce pressure drop simultaneously by changing the geometry of the vortex seeker cyclone, especially in large-scale industrial cyclone separators [35]. This is because the vortex finder is a transitional area of circulation flow which has uniform axial velocity on the outside and vortex core flow with dominant tangential velocity on the inside [26]. Based on the literature review presented shows that several innovations to improve the performance of square cyclones. This study focuses on the deformation of the vortex finder as an effective solution to overcome the efficiency of gas particle separator and the decrease in tangential velocity due to the increase in the intake air temperature. The presented results show that using the optimized shape of the vortex finder is a simple and effective method to increase the separation efficiency. Apart from the basic model of the cylindrical vortex finder, there are three different vortex locators, namely the Standard Vortex (SV), Convergent Vortex (CV), Divergent Vortex (DV), and Convergent Divergent Vortex (CDV) vortexes with different shapes and 0.75 outflow sizes and 0.50 will be studied. Computational Fluid Dynamics (CFD) technique was used to determine the effect of flow characteristics in a square cyclone with changes in the shape of the vortex finder. The results of this study are expected to be a theoretical guideline for particle collection technology in a square cyclone separator by involving a vortex finder geometry innovation with different shapes.

II. MATERIALS AND METHODOLOGIES

2.1 Gas Phase Modelling

The gas flow inside the cyclone is in a turbulent flow regime. For incompressible flow the continuity equation is given as follows:

$$\frac{\partial \bar{u}_i}{\partial x_i} = 0 \qquad (1)$$

The momentum equation is:

$$\frac{\partial \bar{u}_i}{\partial x_i} + \bar{u}_j \frac{\partial \bar{u}_i}{\partial x_j} = -\frac{1}{\rho}\frac{\partial \bar{P}}{\partial x_i} + v\frac{\partial^2 \bar{u}_i}{\partial x_j \partial x_j} - \frac{\partial}{\partial x_j} Rij \qquad (2)$$

Where$\bar{u}_i$ and $x_i$each represents the average speed of the coordinate system. In this equation, $\bar{P}$indicates the average pressure, and$Rij = \bar{u}_i \bar{u}_j$is the Reynolds stress form,ρ and $v$show the density of the gas and the kinematic viscosity of the gas, respectively. Here$u'_i = u_i - \bar{u}_i$is the component of fluctuating velocity to$i$. Discrete Phase Model (DPM) from the Ansys-Fluent CFD model was used to evaluate the trajectories of particles in the Lagrangian frame of reference by determining the size and density of individual particles [36].

It should be emphasized that the turbulence model$k-\varepsilon$ standart, RNG $k-\varepsilon$, and Realizable$k-\varepsilon$cannot reliably predict the strong eddies and anisotropic effects of the airflow field in gas cyclones [37] [38]. In a recent study, Reynolds Stress Model (RSM) and Large Eddy Simulation (LES) were more effective in simulating the flow field in a cyclone separator [37] [36]. In a study [39], it was shown that using

International Research Journal of Innovations in Engineering and Technology (IRJIET)

ISSN (online): 2581-3048

Volume 6, Issue 11, pp 12-24, November-2022

https://doi.org/10.47001/IRJIET/2022.611002

the LES model to predict flow in a cyclone gave more accurate results than RSM. However, the use of LES requires a very fine meshing that requires power demand, high computational costs and a long time. Nonetheless, RSM can provide nearly cyclone performance prediction results with much lower experimental results and computational meshing (due to coarser lattice) than LES. Therefore, RSM was used to solve the turbulent flow field in the gas cyclone in this study.

The last closed RSM transport equation is given as:

$$\frac{\partial}{\partial t}R_{ij} + \bar{u}_k \frac{\partial}{\partial x_k}R_{ij} = \frac{\partial}{\partial x_k}\left(\frac{v_t}{\sigma^k}\frac{\partial}{\partial x_k}R_{ij}\right) - \left[R_{ik}\frac{\partial \bar{u}_j}{\partial x_k} + R_{jk}\frac{\partial \bar{u}_i}{\partial x_k}\right]$$

$$-C_1\frac{\varepsilon}{K}\left[R_{ij} - \frac{2}{3}\delta_{ij}K\right] - C_2\left[P_{ij} - \frac{2}{3}\delta_{ij}P\right] - \frac{2}{3}\delta_{ij}\varepsilon \qquad (3)$$

Where P_{ij} can be written as follows:

$$P_{ij} = -\left[R_{ik}\frac{\partial \bar{u}_j}{\partial x_k} + R_{jk}\frac{\partial \bar{u}_i}{\partial x_k}\right], P_f = \frac{1}{2}P_{ij} \qquad (4)$$

With P_f is fluctuating energy production, $v_t$is turbulent viscosity (eddy), and $\sigma^k = 1$, $C_1 = 1.8, C_2 = 0.6$is an empirical constant. Transport equation for turbulence dissipation rate ε,given as follows:

$$\frac{\partial \varepsilon}{\partial t} + \bar{u}_j\frac{\partial \varepsilon}{\partial x_j} = \frac{\partial}{\partial x_j}\left(v + \frac{v_t}{\sigma^\varepsilon}\frac{\partial \varepsilon}{\partial x_j}\right) - C^{\varepsilon 1}\frac{\varepsilon}{K}R_{ij} - C^{\varepsilon 2}\frac{\varepsilon^2}{K} \qquad (5)$$

In the above equation (5), $K = \frac{1}{2}\overline{u'}_i\overline{u'}_i$ is the fluctuating kinetic energy and represents the turbulence dissipation rate. The constant value is$\sigma^\varepsilon = 1.3, C^{\varepsilon 1} = 1.44, C^{\varepsilon 2} = 1.92$.

2.2 Partikel Phase Modelling

The gas flow of charged particles in a cyclone separator was investigated by the Eulerian-Lagrangian method. In this CFD simulation, the approach is implemented in a discrete phase model (DPM) where the solid phase and the fluid phase are implemented, respectively, as discrete and continuous phases. Since the discrete phase has a low volume fraction, one way coupling method is used and particle collisions are ignored [40]. The drag coefficient for spherical particles was calculated according to the method of Morsi and Alexander [41]. A Discrite Random Walk (DRW) model was also applied to account for the effect of fluctuating airflow turbulence on the particles [36].

The equation of motion of the particle is given as follows:

$$\frac{\partial u_{pi}}{dt} = \frac{18\mu}{\rho_p d_p^2}\frac{C_D Re_p}{24}\left(u_i - u_{pi}\right) + \frac{g_i(\rho_p - \rho)}{\rho_p} \qquad (6)$$

$$\frac{\partial x_{pi}}{dt} = u_{pi} \qquad (7)$$

ρ_p and d_p respectively according to the density and diameter of the particles. C_D show drag coefficient, u_i and u_{pi} represent the gas and particle velocities in the direction, respectively$i$, and show dynamic viscosity and gas density, respectively. g_i is the acceleration due to gravity in the direction$i$and$Re_p$is the relative Reynolds number.

$$Re_p = \frac{\rho_p d_p |u - u_p|}{\mu} \qquad (8)$$

2.3 Cyclone Geometry

In this study, a comprehensive investigation of the effect of vortex finder geometry on square cyclone performance uses the CFD approach. Four variations of different geometric shapes in the vortex finder shape, namely cylinder, convergent, divergent and convergent divergent vortex finder. The shape of the vortex finder in this study is almost similar to the study [35], where in his study varied the length of the vortex finder with a convergent shape. It should be noted that in this study a square cyclone does not changes and only the shape of the vortex finder varies. Figure 1. Shows the geometry of a square cyclone with a single inlet section as a consideration in this study. In this case, the vortex finder is in the center of the upper body of the cyclone according to the design of the experimental study of the study [42], while for the geometry of the cyclone the diameter follows that of the study [29]. The coordinate system is set at the bottom and the dimensions of the shape of the cyclone separator can be seen in Figure 2. The center axis of the cyclone is defined as the z-axis with an upward direction. The overall geometric dimensions of the cyclone for all variation cases are presented in Table 1.

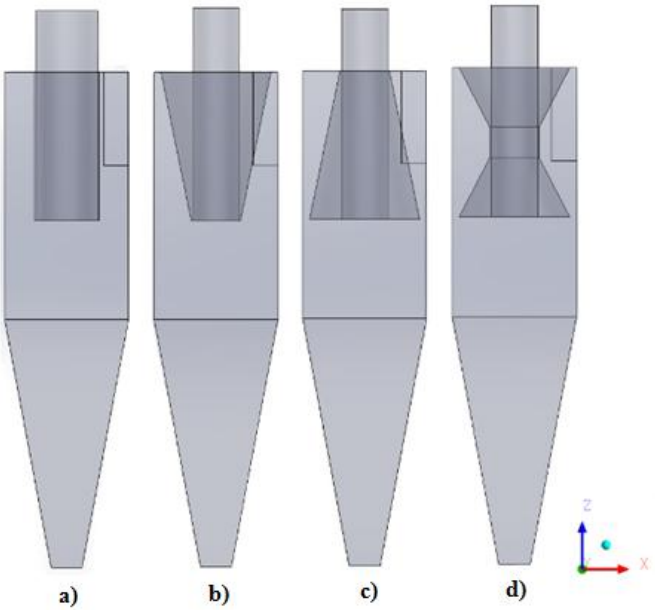

Figure 1: Square cyclone with a) Cylindrical, b) Convergent, c) Divergent, and d) Convergent Divergent vortex finder

International Research Journal of Innovations in Engineering and Technology (IRJIET)
ISSN (online): 2581-3048
Volume 6, Issue 11, pp 12-24, November-2022
https://doi.org/10.47001/IRJIET/2022.611002

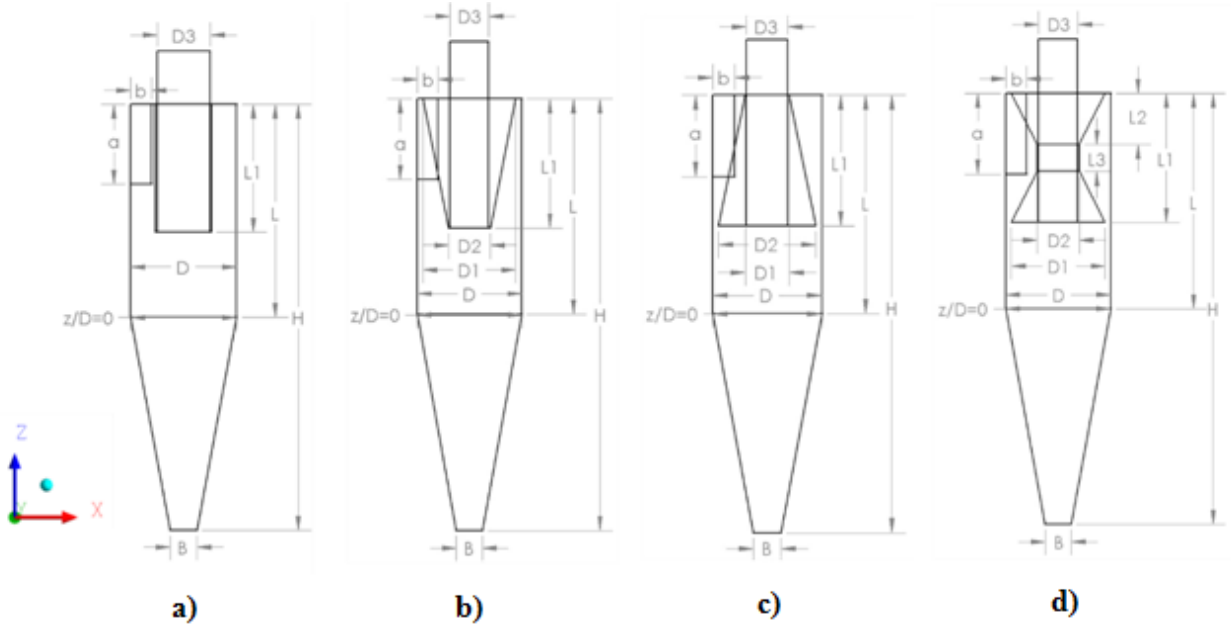

Figure 2: Dimensions of the cyclone separator a) Cylindrical, b) Convergent, c) Divergent, and d) Convergent Divergent vortex finder

Table 1: Dimensions of the square cyclone (D = 200 mm)

Dimensions	D1	D2	D3	a/D	b/D	L3/D	L2/D	L1/D	L/D	H/D	B/D
Cylindrical vortex finder	-	-	0.5	0.75	0.2	-	-	1.2	2	4	0.25
Convergen vortex finder	0.89	0.4	0.375 0.25	0.75	0.2	-	-	1.2	2	4	0.25
Divergen vortex finder	0.4	0.89	0.375 0.25	0.75	0.2	-	-	1.2	2	4	0.25
ConvergenDivergen vortex finder	0.89	0.4	0.375 0.25	0.75	0.2	0.25	0.475	1.2	2	4	0.25

2.4 Grid Independence Study

In this study, the cyclone grid uses a hexahedral structure generated by the commercial software ANSYS-ICEM CFD which can be seen as shown in Figure 3. The determination of the appropriate grid is one of the most substantial factors affecting the accuracy of the numerical simulation. An independent grid study was conducted to obtain the appropriate grid resolution. Determination of a good grid can be seen from the quality of the Determinants in ICEM more than 0.2. The grid approach was tested using five independent grid levels, namely, 400,000, 500,000, 600,000, 700,000, and 800,000 cells, this was done to obtain accurate numerical results. Static pressure on $z/D = 0{,}75$ for incoming air velocity $12\,m/s$ can be illustrated in Figure 4. Each grid is compared to the computational results of the medium grid and the smoothest grid, resulting in an error of 3%.

However, a grid of 600,000 cells was applied to all simulation cases to ensure the accuracy of the computational results. The following is the design of the cyclone variation in this study.

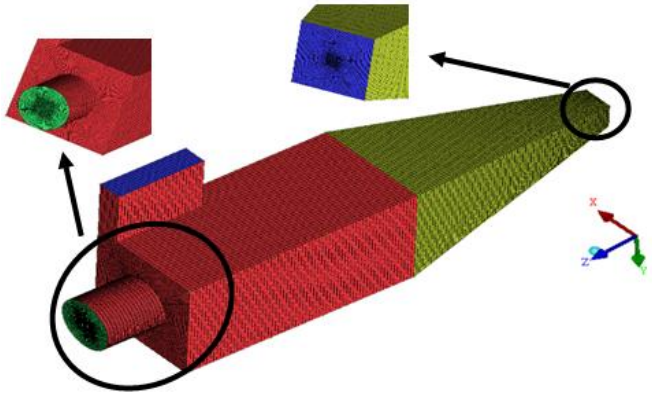

Figure 3: Numerical Grid

International Research Journal of Innovations in Engineering and Technology (IRJIET)
ISSN (online): 2581-3048
Volume 6, Issue 11, pp 12-24, November-2022
https://doi.org/10.47001/IRJIET/2022.611002

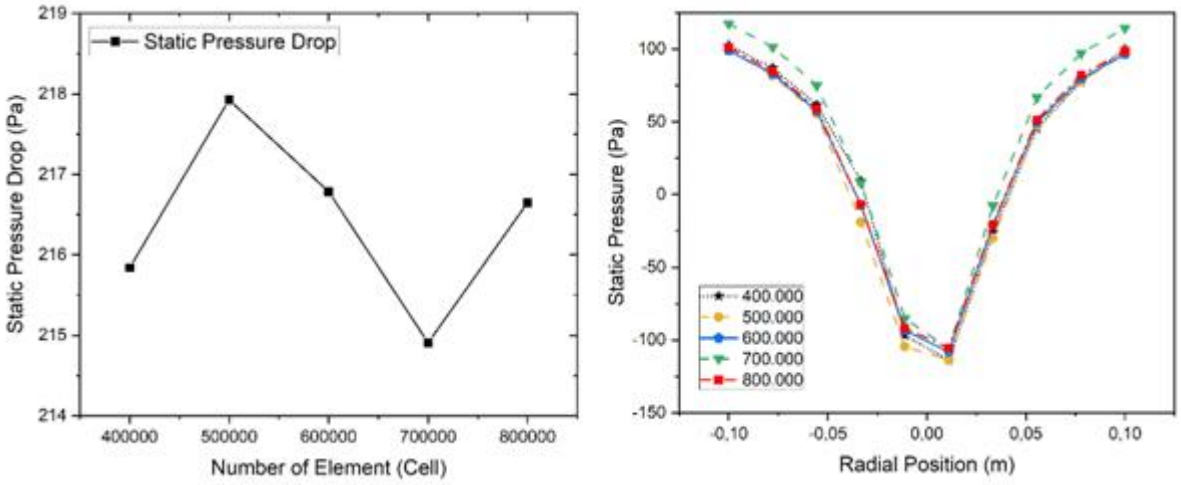

Figure 4: Grid independence test in terms of (a) pressure drop (b) static pressure profile at site $z/D = 0,75$

2.5 Boundary Conditions dnd Solver Setting

The entry speed in this study is$12 - 28\ m/s$. The intake air is assumed to flow uniformly into a square cyclone from the inlet side, and at the outflow section it is regulated as a gas outflow. On the inlet side, the temperature is set at 293, 350, 500 and 700 K with an inlet speed of only$12\ m/s$. In addition to the entry and exit sides, they are treated as walls, where a "no-slip" wall boundary condition is applied. The DPM "trap" condition is assumed at the outlet side of the dustbin. The particles are assumed to enter the gas cyclone through the inlet side at the same speed as the gas velocity. In this CFD simulation, 10,000 tea particles enter from the Fluidized Bed Dryer (FBD) in a tea dryer with a density of$1989,7\ kg/m^3$and fed into the gas cyclone from the inlet. Particle diameters range from 1 to$32\ m$. The density and viscosity of air are$1,225\ kg/m^3$and $1,7894 \times 10^{-5} kg/ms$.The standard wall functions are utilized for all solid walls of the square cyclone.

To analyze several cases of cyclone separator variation, the ANSYS Fluent 20 R1 CFD was used to computationally investigate the flow in a square cyclone. The volume average and URANS equations are solved numerically using the Finite Volume Method (FVM) approach. Turbulence intensity is obtained from speed$12\ m/s$is[41,10]considered as 4%, and the hydraulic diameter is$0,063\ m$in the inlet. The detailed CFD simulation settings are shown in Table 2. The simulation starts with steady solver conditions for 10,000 iterations (gas only) and then switches to unsteady (by including particle tracking) with a time step10^{-4} s. residence time depends on the volume of the cyclone and the volumetric flow rate of the gas [43]. The time step considered in the CFD simulation is sufficient from the lowest cyclone residence time.

Table 2: Numerical settings

Model condition	Model setting
Turbulence	Reynolds stress model (RSM)
Solution method	Pressure velocity coupling: SIMPLEC
	Pressure: PRESTO!
	Momentum: Quick
	Turbulent kinetic energy: second-order upwind
	Specific dissipation rate: Second-order upwind
	Reynolds stresses: First-order upwind

III. RESULT AND DISCUSSION

3.1 Validation Section

To find out the results of the accuracy of the computational simulation, the validation of the predicted results from experimental and numerical data. In Figure 5, the CFD results for tangential velocity and pressure drop are compared with experimental and numerical data from [42] and from research numerical data [29]. Meanwhile, the validation temperature data was compared from the research [26]. As from the results that have been shown, the CFD results predict the tangential velocity and pressure drop from the experimental results obtained with good results.

International Research Journal of Innovations in Engineering and Technology (IRJIET)
ISSN (online): 2581-3048
Volume 6, Issue 11, pp 12-24, November-2022
https://doi.org/10.47001/IRJIET/2022.611002

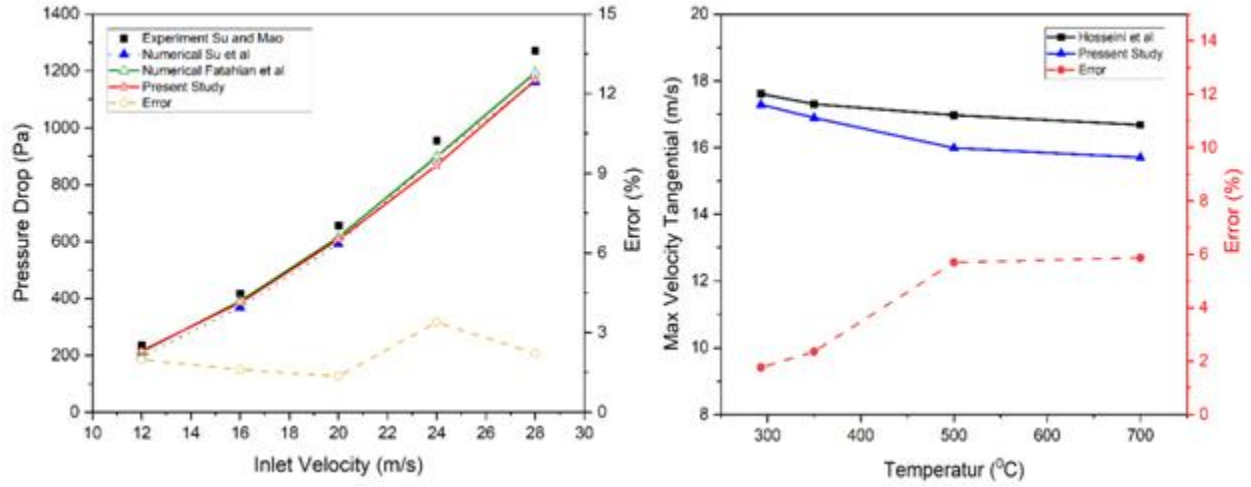

Figure 5: Comparison of predictions a) Pressure drop b) Inlet heat temperature with previous research experiments

3.2 Effect of Vortex Finder on the Flow Field

3.2.1 Tangential Velocity

On the graph of the cyclone the results of the static pressure with the inlet velocity 12 m/sshows that the tangential velocity profile has two different results. The inside of the flow of the gas vortex forming a V shape is called the forced vortex. The tangential velocity in the forced vortex area continuously increases radially until it reaches a maximum point and decreases again in the outer region of the vortex or near the cyclone wall. This distribution is defined as a Rankine-type vortex [44].

Tangential velocity is an important velocity component in particle separation because this velocity directly affects the centrifugal force and efficiency of the gas separator cyclone. The higher the value of the centrifugal force, the higher the particles collected. Figures 6 and 7 show the tangential velocity contours on the plane$z/D = 0{,}75$on the variation of the shape of the vortex finder with outflow diameter 0.375 and outflow diameter 0.25. The contour represents the rankine vortex which consists of two parts, namely free vortex and force vortex. Free eddy flow has the characteristics of frictionless rotating flow. The tangential velocity in this flow has the same fluid momentum moment for each radius of rotation. In contrast, forced eddy flow has the same tangential velocity distribution as the rotation of the solid. In some variations the shape of the vortex finder as shown in Fig. 7 there is a negative tangential velocity. This is due to the Processing Vortex Core (PVC) phenomenon, namely the occurrence of oscillations in the vortex core on the rotating axis of the cyclone geometry [21]. To get clearer results, the data is presented in the form of a tangential velocity distribution graph. Research to investigate the performance of this cyclone is expected that the value of the tangential velocity increases along with the pressure drop which also increases due to strong coupling.

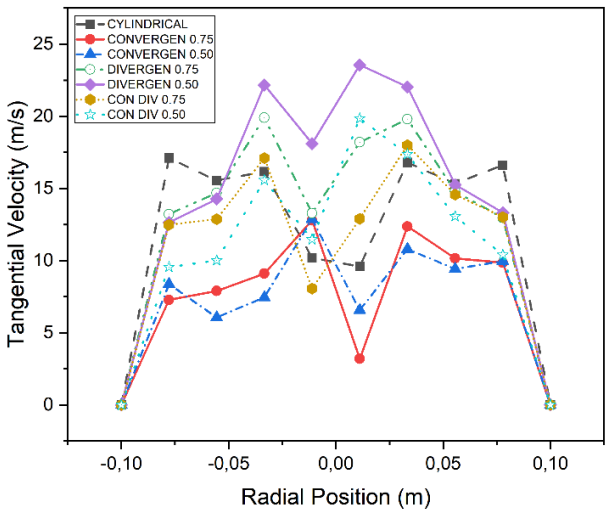

Figure 6: Effect of the shape of the vortex finder on the tangential velocity at the location $z/D = 0,75$(under the vortex finder)

International Research Journal of Innovations in Engineering and Technology (IRJIET)
ISSN (online): 2581-3048
Volume 6, Issue 11, pp 12-24, November-2022
https://doi.org/10.47001/IRJIET/2022.611002

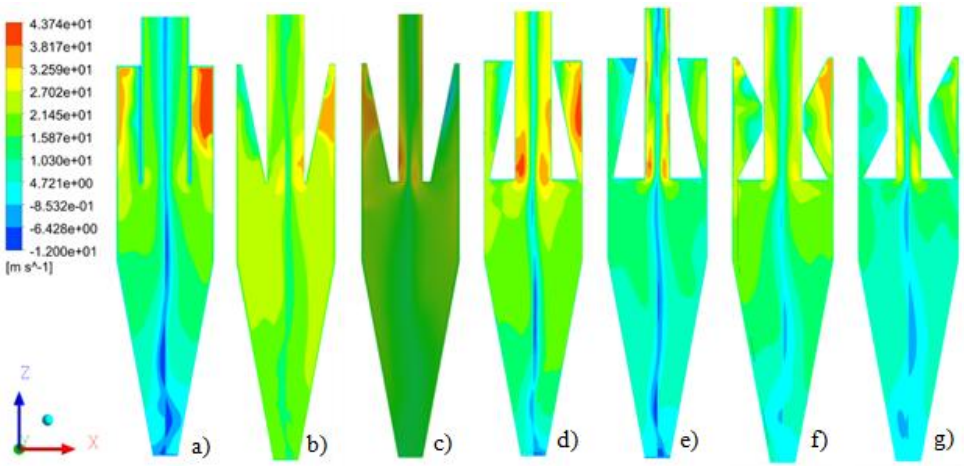

Figure 7: Tangential velocity contour at location z/D=0.75 (below the vortex finder) a) cylinder, b) Convergent 0.75, c) Convergent 0.50, d) Divergent 0.75, e) Divergent 0.50, f) Convergent Divergent 0.75 , g) Convergent Divergent 0.50

In Figure 7, seen from the overall contour of the vortex finder, the cyclone wall becomes zero due to frictional forces from the opposite direction. The tangential velocity in the forced vortex area increases radially until it reaches the peak point and then decreases following the radius in the free vortex region [45]. Tangential velocity has a shape similar to an inverted W. In the area below the graph the divergent shape increases as the outflow diameter decreases. Picture 7 also shows the highest tangential velocity achieved in the cyclone model when the shape of the vortex finder is modified to diverge and the outflow diameter size is 0.25.

3.2.2 Pressure static

Pressure drop is a cyclone performance parameter indicating the amount of energy required to move particles through the system. The pressure drop is a function of the inlet gas velocity and the cyclone diameter [2]. Usually, the greatest pressure drop occurs in the body due to eddies and energy dissipation. The pressure drop is calculated by comparing the pressure gap between the inlet and outlet. Empirically the relationship between pressure loss and gas intake velocity can be written in Eq. (28) [43]:

$$\Delta P = \xi \frac{\rho V_{in}{}^2}{2} \qquad (9)$$

Where ξ is the pressure loss coefficient and V_{in} is the gas intake velocity. The effect of the shape of the vortex finder and the diameter of the outflow on the cyclone body can be observed in this section.

Picture 8 and 9 show that modifying the vortex finder can increase the pressure drop. At first the particles will enter through the inlet tangentially. The shape of the cyclone body will produce a vortex flow. Particles will rotate according to geometric shapes.

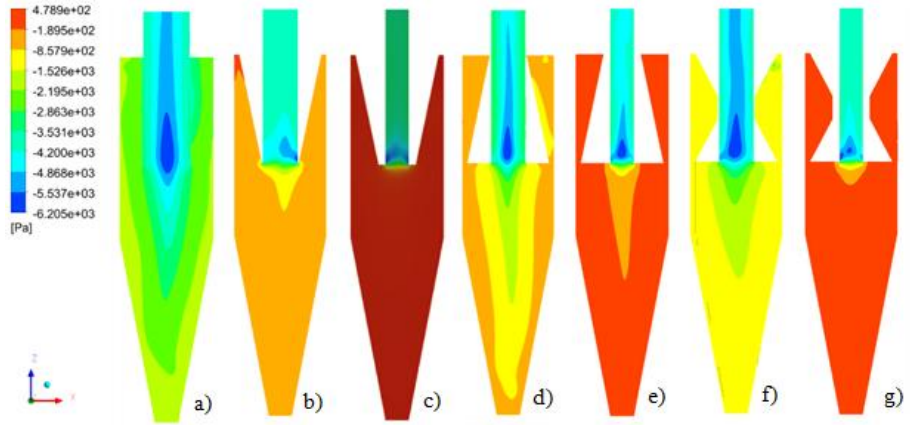

Figure 8: Contour of static pressure at location z/D=0.75 (below the vortex finder) a) cylinder, b) Convergent 0.75, c) Convergent 0.50, d) Divergent 0.75, e) Divergent 0.50, f) Convergent Divergent 0.75 , g) Convergent Divergent 0.50

International Research Journal of Innovations in Engineering and Technology (IRJIET)
ISSN (online): 2581-3048
Volume 6, Issue 11, pp 12-24, November-2022
https://doi.org/10.47001/IRJIET/2022.611002

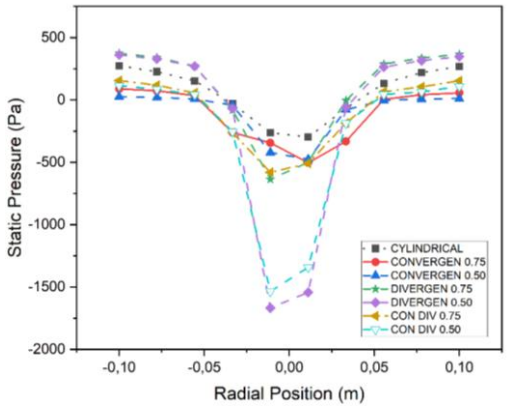

Figure 9: Effect of the shape of the vortex finder on the static pressure at the site $z/D = 0,75$ (under the vortex finder)

Cyclone and during that rotation, friction occurs with the walls of the cyclone. In the concept of fluid mechanics, this friction will cause a no slip condition, where the pressure around the wall is greater than the center of the cyclone, as a result the pressure gradient on the cyclone is dominant in the radial direction. The static pressure reaches its maximum value in the wall area and decreases radially towards the center of the geometry. This is in line with research conducted by Ficici et al. [46], Raoufi et al. [47], and Fu et al. [48].

The effect of the modified divergent model with an outflow diameter of 0.50 gives significant results. This can be observed in the static pressure contour in Fig. 8 and 9 that the static pressure value gradually decreases in the 0.50 outflow diameter divergent model which is characterized by a color change from the high pressure area to the low pressure area (red to orange to yellow). The pressure drop of the 0.50 outflow diameter divergent model decreased to 39% when compared to the 0.50 outflow diameter model without convergence. This is the advantage of the cyclone model in terms of energy consumption.

Based on Figure 9 the graph of static pressure has similarities to the V shape. This shape is based on the distribution of static pressure which has low values in the middle and high in the wall area due to cyclonic friction. Modifying the shape of the vortex finder has an effect on increasing the pressure drop. However, the combination of the innovative shape of the vortex finder and the outflow diameter of the cyclone has succeeded in reducing the pressure drop. It can be seen in the graph that there is a decrease in inlet pressure from 375 Pa to 88.9 Pa. As a result, the divergent model can reduce the flow resistance in the vortex finder following the kinetic movement of gas particles coupled with a reduced outflow diameter [49] so that the flow becomes more uniform which has an impact on the pressure drop [50].

3.2.3 Turbulen intensity

For inlet velocity $v = 12\ m/s$, Picture 10 and 11 compare the turbulence intensity profile on $z/D = 0{,}75$in a square cyclone with a different vortex finder. The corresponding turbulence intensity contours for all square cyclones are presented in Fig. 11. For all cyclones with different vortex finder, relatively stable flow appears in the cone section with rather low turbulence intensity. The maximum turbulence intensity is seen near the sidewall and bottom of the vortex finder.

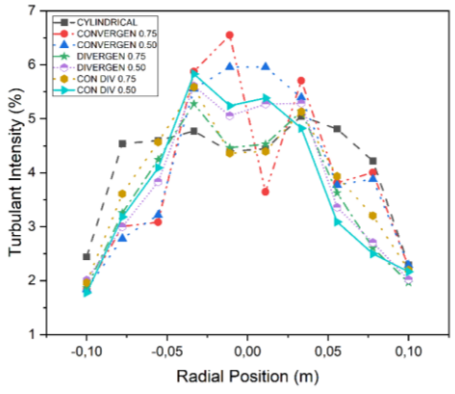

Figure 10: Effect of fortex finder shape and outflow diameter on turbulence intensity profile

International Research Journal of Innovations in Engineering and Technology (IRJIET)
ISSN (online): 2581-3048
Volume 6, Issue 11, pp 12-24, November-2022
https://doi.org/10.47001/IRJIET/2022.611002

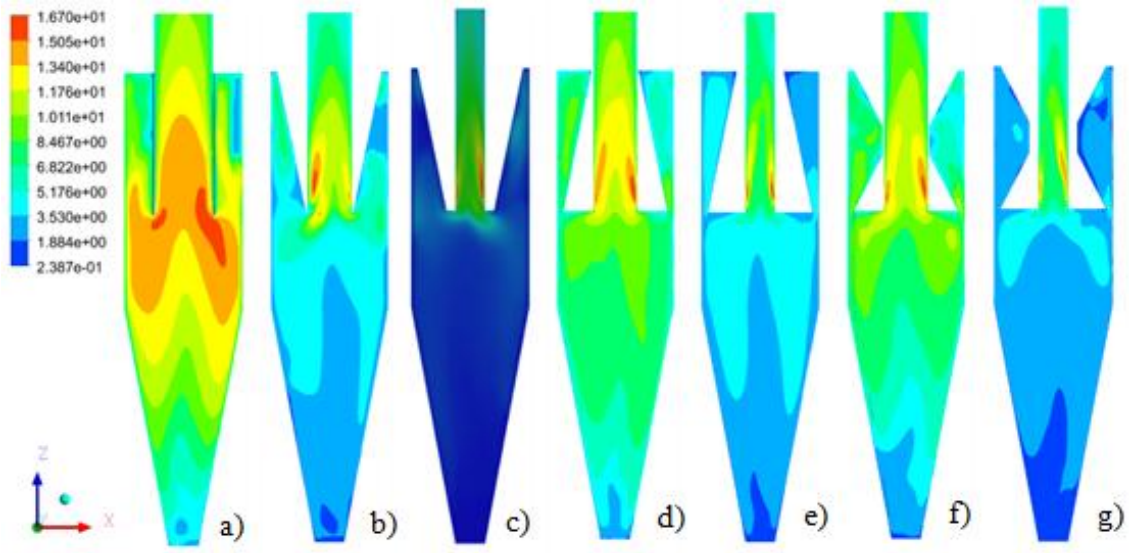

Figure 11: Contour of turbulence intensity in a square cyclone with a) cylinder, b) Convergent 0.75, c) Convergent 0.50, d) Divergent 0.75, e) Divergent 0.50, f) Convergent Divergent 0.75, g) Convergent Divergent 0.50

The high level of turbulence in the area near the vortex finder has a negative impact on the separation efficiency. This is because turbulence can drag particles into the vortex seeker and cause them to escape along with the gas. Although the turbulence intensity is higher in the convergent vortex seeker, it does not affect the separation efficiency. This is because most of the particles are separated in the outer vortex area due to the high degree of centrifugal force in this region. This behavior was also reported by Pei et al. [50].

Both the diameter and length of the vortex finder affect the turbulence intensity of the square cyclone. Comparing the results reveals that using a convergent vortex finder decreases the turbulence intensity in the outer vortex region. The smaller size of the vortex finder diameter ratio causes lower turbulence intensity in the cyclone airflow field. Xiaodong et al. [51] reported that increasing turbulence intensity reduces the separation efficiency of a larger cyclone separator (divergent vortex finder) increases turbulence intensity near the wall compared to a convergent vortex finder and will decrease separation efficiency. Therefore, it is expected that the separation efficiency of a square cyclone with a convergent vortex seeker will be higher than that of other cyclones. Figure 11 shows that the convergent vortex finder produces the highest turbulence intensity in most of the cyclones, while the convergent vortex finder produces the lowest turbulence intensity in the square cyclone.

3.2.4 Separation Efficiency

Picture Fig. 12 shows the effect of the ratio of the shape of the vortex finder and the diameter of the outflow on the separation efficiency of a square cyclone for inlet velocities of 12 and 20 m/s. The separation efficiency was calculated by tracking the particles released from the inlet section using the DPM model. The cyclone efficiency for a particle of a given diameter can be written as:

$$\text{Separation efficiency} = \frac{number\ \ of\ released\ \ particles\ -number\ \ of\ escaped\ \ particles}{number\ \ of\ released\ \ particles} \qquad (10)$$

These figures show that the separation efficiency increases with increasing inlet velocity for all square cyclones. In addition, the use of the convergent vortex finder greatly improves the separation efficiency of the square cyclone at both inlet speeds. This is because replacing the cylindrical vortex finder with a converging one increases the tangential velocity which increases the separation efficiency. The CFD results also show that changes in the outflow diameter affect the separation efficiency. The highest separation efficiency value was obtained for the convergent vortex finder 0.75 and the lowest for the convergent divergent vortex finder 0.50.

International Research Journal of Innovations in Engineering and Technology (IRJIET)

ISSN (online): 2581-3048

Volume 6, Issue 11, pp 12-24, November-2022

https://doi.org/10.47001/IRJIET/2022.611002

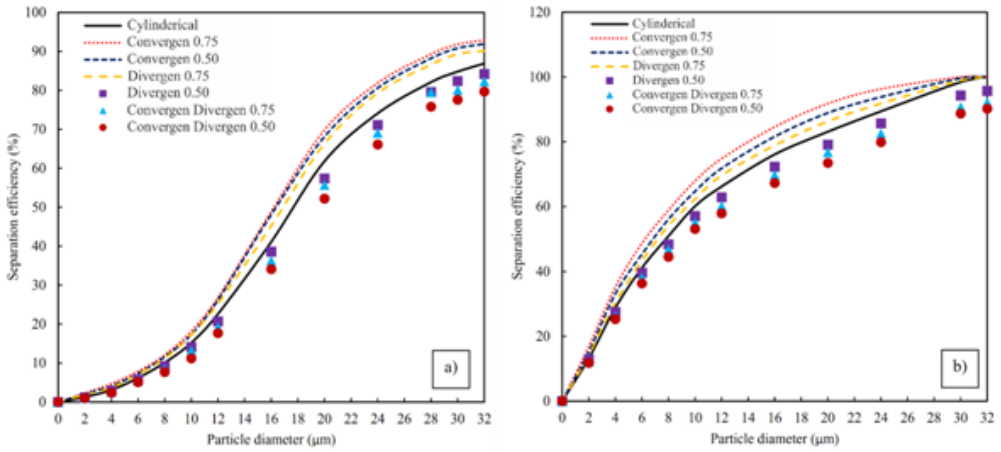

Figure 12: Comparison of the efficiency of a square cyclone separator with modified vortex finder shape and outflow diameter for a) 12 m/s and b) 20 m/s speeds

It can be seen from Figure 12 that the 0.75 convergent vortex finder shows the best performance among all the vortex finder. Although all convergent divergent vortex finders produce lower separation efficiency than cylinders, 0.75 divergent vortex finders perform better than cylindrical and convergent vortex finders.

IV. CONCLUSION

This research computationally studies the effect of different vortex finder shapes and outflow diameters on the internal gas flow plane and the separation performance of square cyclones. The effect of the three shapes of the vortex finder was analyzed through a series of 3D CFD simulations. The unstable RANS equations, including the Reynolds Stress Turbulence Model and the Eulerian-Lagrangian approximation, were used to simulate airflow and particle dynamics in gas cyclones.

The main conclusion of this research is

1. The shape of the vortex finder is important and significantly affects the pattern and performance of the square cyclone gas flow
2. Divergent vortex finder increases the pressure in the free vortex region, followed by divergent convergence compared to other forms of vortex finder.
3. The shape of the vortex finder affects the tangential velocity in a square cyclone. The maximum tangential velocity occurs near the vortex finder.
4. A maximum tangential velocity of about 3.56 times the inlet velocity was obtained for a square cyclone with a divergent vortex finder shape with an outflow diameter of 0.50 for an inlet velocity of 20 m/s. The divergent vortex finder is able to increase the tangential velocity by up to 40% in relation to the maximum tangential velocity of a square cyclone with a cylindrical vortex finder.
5. Cyclone separation efficiency and pressure drop are significantly affected by modifying the shape of the vortex finder.
6. The particle separation efficiency increased significantly for the convergent vortex finder reaching 42% but was associated with a significant increase in pressure drop of up to 24% for the 0.75 outflow diameter.

Statement of Competing Interests

The authors state that they are not aware of any competing financial interests or personal relationships that are likely to influence the work reported in this paper.

REFERENCES

[1] M. Rhodes, Introduction to Particle Technology, *John Wiley and Sons, West Sussex, England*, 2008.

[2] L. Theodore, Air Pollution Controll Equipment, *John Wiley and Sons, New Jersey, Canada*, 2008.

[3] L. J. Graham, R. Taillon, J. Mullin, and T. Wigle, "Pharmaceutical process/equipment design methodology case study: Cyclone design to optimize spray-dried-particle collection efficiency," *Comput. Chem. Eng.*, vol. 34, no. 7, pp. 1041–1048, Jul. 2010, doi: 10.1016/j.compchemeng.2010.04.004.

[4] V. Kumar and K. Jha, "Multi-objective shape optimization of vortex finders in cyclone separators using response surface methodology and genetic algorithms," *Sep. Purif. Technol.*, vol. 215, no. October 2018, pp. 25–31, 2019, doi: 10.1016/j.seppur.2018.12.083.

[5] I. Karagoz, A. Avci, A. Surmen, and O. Sendogan, "Design and performance evaluation of a new cyclone separator," *J. Aerosol Sci.*, vol. 59, pp. 57–64, 2013, doi: 10.1016/j.jaerosci.2013.01.010.

ISSN (online): 2581-3048
Volume 6, Issue 11, pp 12-24, November-2022
https://doi.org/10.47001/IRJIET/2022.611002

[6] L. S. Brar, R. P. Sharma, and R. Dwivedi, "Effect of vortex finder diameter on flow field and collection efficiency of cyclone separators," *Part. Sci. Technol.*, vol. 33, no. 1, pp. 34–40, 2015, doi: 10.1080/02726351.2014.933144.

[7] J. Feng, W. Chen, L. Wang, and X. Peng, "Separation performance of new type of multi-stage axial cyclone used as demister in power plant emission system," *J. Dispers. Sci. Technol.*, vol. 41, no. 11, pp. 1643–1656, 2020, doi: 10.1080/01932691.2019.1634584.

[8] J. Duan, S. Gao, Y. Lu, W. Wang, P. Zhang, and C. Li, "Study and optimization of flow field in a novel cyclone separator with inner cylinder," *Adv. Powder Technol.*, vol. 31, no. 10, pp. 4166–4179, 2020, doi: 10.1016/j.apt.2020.08.020.

[9] K. Elsayed and C. Lacor, "Numerical modeling of the flow field and performance in cyclones of different cone-tip diameters," *Comput. Fluids*, vol. 51, no. 1, pp. 48–59, 2011, doi: 10.1016/j.compfluid.2011.07.010.

[10] B. Zhao, Y. Su, and J. Zhang, "Simulation of gas flow pattern and separation efficiency in cyclone with conventional single and spiral double inlet configuration," *Chem. Eng. Res. Des.*, vol. 84, no. 12 A, pp. 1158–1165, 2006, doi: 10.1205/cherd06040.

[11] E. Fatahian, H. Fatahian, E. Hosseini, and G. Ahmadi, "A low-cost solution for the collection of fine particles in square cyclone: A numerical analysis," *Powder Technol.*, vol. 387, pp. 454–465, 2021, doi: 10.1016/j.powtec.2021.04.048.

[12] Q. Zhao, B. Cui, D. Wei, T. Song, and Y. Feng, "Numerical analysis of the flow field and separation performance in hydrocyclones with different vortex finder wall thickness," *Powder Technol.*, vol. 345, pp. 478–491, 2019, doi: 10.1016/j.powtec.2019.01.030.

[13] E. Yohana, M. Tauviqirrahman, B. Yusuf, K. H. Choi, and V. Paramita, "Effect of vortex limiter position and metal rod insertion on the flow field, heat rate, and performance of cyclone separator," *Powder Technol.*, vol. 377, pp. 464–475, 2021, doi: 10.1016/j.powtec.2020.09.014.

[14] W. D. Griffiths and F. Boysan, "Computational fluid dynamics (CFD) and empirical modelling of the performance of a number of cyclone samplers," *J. Aerosol Sci.*, vol. 27, no. 2, pp. 281–304, 1996, doi: 10.1016/0021-8502(95)00549-8.

[15] K. Elsayed and C. Lacor, "The effect of the dust outlet geometry on the performance and hydrodynamics of gas cyclones," *Comput. Fluids*, vol. 68, pp. 134–147, 2012, doi: 10.1016/j.compfluid.2012.07.029.

[16] E. Yohana, M. Tauviqirrahman, B. Yusuf, K. H. Choi, and V. Paramita, "Effect of vortex limiter position and metal rod insertion on the flow field, heat rate, and performance of cyclone separator," *Powder Technol.*, vol. 377, pp. 464–475, 2021, doi: 10.1016/j.powtec.2020.09.014.

[17] T. Mothilal, K. Pitchandi, V. Velukumar, and K. Parthiban, "CFD and statistical approach for optimization of operating parameters in a tangential cyclone heat exchanger," *J. Appl. Fluid Mech.*, vol. 11, no. 2, pp. 459–466, 2018, doi: 10.29252/jafm.11.02.27791.

[18] G. Gronald and J. J. Derksen, "Simulating turbulent swirling flow in a gas cyclone: A comparison of various modeling approaches," *Powder Technol.*, vol. 205, no. 1–3, pp. 160–171, 2011, doi: 10.1016/j.powtec.2010.09.007.

[19] A.Horvath, C. Jordan, and M. Harasek, "Influence of vortex-finder diameter on axial gas flow in simple cyclone," *Chem. Prod. Process Model.*, vol. 3, no. 1, 2008, doi: 10.2202/1934-2659.1149.

[20] F. Kaya, I. Karagoz, and A. Avci, "Effects of surface roughness on the performance of tangential inlet cyclone separators," *Aerosol Sci. Technol.*, vol. 45, no. 8, pp. 988–995, 2011, doi: 10.1080/02786826.2011.574174.

[21] L. S. Brar, R. P. Sharma, and K. Elsayed, "The effect of the cyclone length on the performance of Stairmand high-efficiency cyclone," *Powder Technol.*, vol. 286, pp. 668–677, 2015, doi: 10.1016/j.powtec.2015.09.003.

[22] J. Duan, S. Gao, Y. Lu, W. Wang, P. Zhang, and C. Li, "Study and optimization of flow field in a novel cyclone separator with inner cylinder," *Adv. Powder Technol.*, vol. 31, no. 10, pp. 4166–4179, 2020, doi: 10.1016/j.apt.2020.08.020.

[23] S. K. Shukla, P. Shukla, and P. Ghosh, "Evaluation of numerical schemes using different simulation methods for the continuous phase modeling of cyclone separators," *Adv. Powder Technol.*, vol. 22, no. 2, pp. 209–219, 2011, doi: 10.1016/j.apt.2010.11.009.

[24] S. K. Shukla, P. Shukla, and P. Ghosh, "The effect of modeling of velocity fluctuations on prediction of collection efficiency of cyclone separators," *Appl. Math. Model.*, vol. 37, no. 8, pp. 5774–5789, 2013, doi: 10.1016/j.apm.2012.11.019.

[25] Q. Wei, G. Sun, and C. Gao, "Numerical analysis of axial gas flow in cyclone separators with different vortex finder diameters and inlet dimensions," *Powder Technol.*, vol. 369, pp. 321–333, 2020, doi: 10.1016/j.powtec.2020.05.038.

[26] E. Hosseini, H. Fatahian, G. Ahmadi, M. Eshagh Nimvari, and E. Fatahian, "CFD study on the effect of gas temperature on the separation efficiency of square cyclones," *J. Brazilian Soc. Mech. Sci. Eng.*, vol. 43,

ISSN (online): 2581-3048
Volume 6, Issue 11, pp 12-24, November-2022
https://doi.org/10.47001/IRJIET/2022.611002

no. 9, pp. 1–13, 2021, doi: 10.1007/s40430-021-03165-4.

[27] S. Wang, M. Fang, Z. Luo, X. Li, M. Ni, and K. Cen, "Instantaneous separation model of a square cyclone," *Powder Technol.*, vol. 102, no. 1, pp. 65–70, 1999, doi: 10.1016/S0032-5910(98)00196-X.

[28] Y. Su, A. Zheng, and B. Zhao, "Numerical simulation of effect of inlet configuration on square cyclone separator performance," *Powder Technol.*, vol. 210, no. 3, pp. 293–303, 2011, doi: 10.1016/j.powtec.2011.03.034.

[29] H. Fatahian, E. Fatahian, M. Eshagh Nimvari, and G. Ahmadi, "Novel designs for square cyclone using rounded corner and double-inverted cones shapes," *Powder Technol.*, vol. 380, pp. 67–79, 2021, doi: 10.1016/j.powtec.2020.11.034.

[30] N. Malahayati, D. Darmadi, C. Alisa Putri, L. Mairiza, W. Rinaldi, and Y. Yunardi, "Comparative performance analysis between conventional and square cyclones for solid Particle-Gas Separation: A review," *Mater. Today Proc.*, no. xxxx, 2022, doi: 10.1016/j.matpr.2022.03.157.

[31] Y. Su and Y. Mao, "Experimental study on the gas-solid suspension flow in a square cyclone separator," *Chem. Eng. J.*, vol. 121, no. 1, pp. 51–58, 2006, doi: 10.1016/j.cej.2006.04.008.

[32] J. Haake, T. Oggian, J. Utzig, L. M. Rosa, and H. F. Meier, "Investigation of the pressure drop increase in a square free-vortex cyclonic separator operating at low particle concentration," *Powder Technol.*, vol. 374, pp. 95–105, 2020, doi: 10.1016/j.powtec.2020.07.008.

[33] M. Wasilewski, L. S. Brar, and G. Ligus, "Experimental and numerical investigation on the performance of square cyclones with different vortex finder configurations," *Sep. Purif. Technol.*, vol. 239, no. January, pp. 10–24, 2020, doi: 10.1016/j.seppur.2020.116588.

[34] S. Venkatesh, S. P. Sivapirakasam, M. Sakthivel, S. Ganeshkumar, M. Mahendhira Prabhu, and M. Naveenkumar, "Experimental and numerical investigation in the series arrangement square cyclone separator," *Powder Technol.*, vol. 383, pp. 93–103, 2021, doi: 10.1016/j.powtec.2021.01.031.

[35] E. Yohana, M. Tauviqirrahman, D. A. Laksono, H. Charles, K. H. Choi, and M. E. Yulianto, "Innovation of vortex finder geometry (tapered in-cylinder out) and additional cooling of body cyclone on velocity flow field, performance, and heat transfer of cyclone separator," *Powder Technol.*, vol. 399, 2022, doi: 10.1016/j.powtec.2022.117235.

[36] K. Elsayed, F. Parvaz, S. H. Hosseini, and G. Ahmadi, "Influence of the dipleg and dustbin dimensions on performance of gas cyclones: An optimization study," *Sep. Purif. Technol.*, vol. 239, no. January, 2020, doi: 10.1016/j.seppur.2020.116553.

[37] G. Wan, G. Sun, X. Xue, and M. Shi, "Solids concentration simulation of different size particles in a cyclone separator," *Powder Technol.*, vol. 183, no. 1, pp. 94–104, 2008, doi: 10.1016/j.powtec.2007.11.019.

[38] M. Nakhaei, B. Lu, Y. Tian, W. Wang, K. Dam-Johansen, and H. Wu, "CFD modeling of gas-solid cyclone separators at ambient and elevated temperatures," *Processes*, vol. 8, no. 2, pp. 1–26, 2020, doi: 10.3390/pr8020228.

[39] H. I. Erol, O. Turgut, and R. Unal, "Experimental and numerical study of Stairmand cyclone separators: a comparison of the results of small-scale and large-scale cyclones," *Heat Mass Transf. und Stoffuebertragung*, vol. 55, no. 8, pp. 2341–2354, 2019, doi: 10.1007/s00231-019-02589-y.

[40] S. A. Morsi and A. J. Alexander, "An investigation of particle trajectories in two-phase flow systems," *J. Fluid Mech.*, vol. 55, no. 2, pp. 193–208, 1972, doi: 10.1017/S0022112072001806.

[41] Y. Su and Y. Mao, "Experimental study on the gas-solid suspension flow in a square cyclone separator," *Chem. Eng. J.*, vol. 121, no. 1, pp. 51–58, 2006, doi: 10.1016/j.cej.2006.04.008.

[42] F. Parvaz, S. H. Hosseini, K. Elsayed, and G. Ahmadi, "Numerical investigation of effects of inner cone on flow field, performance and erosion rate of cyclone separators," *Sep. Purif. Technol.*, vol. 201, no. February, pp. 223–237, 2018, doi: 10.1016/j.seppur.2018.03.001.

[43] S. Wang, H. Li, R. Wang, X. Wang, R. Tian, and Q. Sun, "Effect of the inlet angle on the performance of a cyclone separator using CFD-DEM," *Adv. Powder Technol.*, vol. 30, no. 2, pp. 227–239, 2019, doi: 10.1016/j.apt.2018.10.027.

[44] A.Raoufi, M. Shams, M. Farzaneh, and R. Ebrahimi, "Numerical simulation and optimization of fluid flow in cyclone vortex finder," *Chem. Eng. Process. Process Intensif.*, vol. 47, no. 1, pp. 128–137, 2008, doi: 10.1016/j.cep.2007.08.004.

[45] F. Ficici, A. Vedat, and M. Kapsiz, "The effects of vortex finder on the pressure drop in cyclone separators," *Int. J. Phys. Sci.*, vol. 5, no. 6, pp. 804–813, 2010.

[46] S. Fu, F. Zhou, G. Sun, H. Yuan, and J. Zhu, "Performance evaluation of industrial large-scale cyclone separator with novel vortex finder," *Adv. Powder Technol.*, vol. 32, no. 3, pp. 931–939, 2021, doi: 10.1016/j.apt.2021.01.033.

ISSN (online): 2581-3048
Volume 6, Issue 11, pp 12-24, November-2022
https://doi.org/10.47001/IRJIET/2022.611002

[47] C. L. Townsend and J. M. Varnum, Fundamentals of Engineering Review. 1986.

[48] B. Pei, L. Yang, K. Dong, Y. Jiang, X. Du, and B. Wang, "The effect of cross-shaped vortex finder on the performance of cyclone separator," *Powder Technol.*, vol. 313, pp. 135–144, 2017, doi: 10.1016/j.powtec.2017.02.066.

[49] G. Wan, G. Sun, X. Xue, and M. Shi, "Solids concentration simulation of different size particles in a cyclone separator," *Powder Technol.*, vol. 183, no. 1, pp. 94–104, 2008, doi: 10.1016/j.powtec.2007.11.019.

[50] L. Xiaodong, Y. Jianhua, C. Yuchun, N. Mingjiang, and C. Kefa, "Numerical simulation of the effects of turbulence intensity and boundary layer on separation efficiency in a cyclone separator," *Chem. Eng. J.*, vol. 95, no. 1–3, pp. 235–240, 2003, doi: 10.1016/S1385-8947(03)00109-8

Citation of this Article:

Abdul Basit, Mohamad Said Kartono Tony Suryo Utomo, Eflita Yohana, Vika Abidah, Kwang-Hwan Choi, "The Effect of Outlet Diameter and Shape of Vortex Finder on the Efficiency of a Square Cyclone" Published in *International Research Journal of Innovations in Engineering and Technology - IRJIET*, Volume 6, Issue 11, pp 12-24, November 2022. Article DOI https://doi.org/10.47001/IRJIET/2022.611002

****

